HVEM is a novel immune checkpoint for prostate cancer immunotherapy in humanized mice

Nicolas Aubert [1*], Simon, Brunel [1*], Daniel Olive [2] and Gilles Marodon [1]

1 Sorbonne Universités, Inserm, CNRS, Centre d'immunologie et maladies infectieuses-Paris, Cimi-Paris, Paris 75013, France

2 Institut Paoli-Calmettes, Aix-Marseille Université, Inserm, CNRS, CRCM, Tumor Immunity Team, IBISA Immunomonitoring platform, Marseille, France (daniel.olive@inserm.fr)

* Equal contributions (nicolas.aubert@inserm.fr, simonbrunel@live.fr)

Corresponding author: Gilles Marodon, gilles.marodon@inserm.fr, Sorbonne Université, Inserm, CNRS, Centre d'immunologie et maladies infectieuses-Paris (CIMI-PARIS), Paris 75013, France

Simple Summary

Prostate cancer is one of the deadliest cancer in which immunotherapy with current immune checkpoint inhibitors have shown limitations. Thus, it is crucial to investigate other checkpoints to determine whether immunotherapy could be feasible to prevent disease progression in prostate cancer patients. Here, we first show that a pair of molecules (HVEM/BTLA) are associated to disease progression in patients. We next show that immunotherapy aimed to target HVEM reduced tumor growth two-fold in vivo in a humanized mice model of the pathology. We determine the mode of action of the therapy to be dependent on CD8+ T cells and associated with improved T cell activation and reduced suppression. We also formally demonstrate that HVEM/BTLA are novel immune checkpoints for the anti-tumor response. Our results indicate that targeting HVEM might be an interesting therapeutic option for prostate cancer patients.

Abstract

The Herpes Virus Entry Mediator (HVEM) delivers a negative signal to T cells mainly through the B and T Lymphocyte Attenuator (BTLA) molecule and thus, could represent a novel immune checkpoint during an

 doi:10.20944/preprints202105.0302.v1

anti-tumor immune response. A formal demonstration that HVEM can be targeted for cancer immunotherapy is however still lacking. Here, we first show that HVEM and BTLA were associated to a worse prognosis in patients with prostate adenocarcinomas, indicating a detrimental role for this pair of molecule during prostate cancer progression. We then show that a monoclonal antibody to human HVEM significantly impacted the growth of a prostate cancer cell line in immuno-compromised NOD.SCID.gc-null mice reconstituted with human T cells. Using CRISPR/Cas9, we showed that HVEM expression by the tumor was mandatory to observe the therapeutic effect. Mechanistically, tumor control was dependent on $CD8^+$ T cells and was associated to an increase in the proliferation and number of tumor-infiltrating leukocytes. Accordingly, the expression of genes belonging to various T cell activation pathways were enriched in tumor infiltrating leukocytes, whereas genes associated with immuno-suppressive pathways were decreased, possibly resulting in modifications of leukocyte adhesion and motility. Finally, we developed a simple *in vivo* assay in humanized mice to directly demonstrate that HVEM was an immune checkpoint for T-cell mediated tumor control. Our results show that targeting HVEM is a promising strategy for prostate cancer immunotherapy.

Keywords: immune checkpoint; HVEM; BTLA; monoclonal antibody; cancer immunotherapy; humanized mice; prostate cancer

Preprints (www.preprints.org) | NOT PEER-REVIEWED | Posted: 13 May 2021 doi:10.20944/preprints202105.0302.v1

Introduction

Immune escape by tumor is now considered a hallmark of cancer [1]. Many immune mechanisms are involved to explain the loss of tumor control, including defective MHC function and expression, recruitment of suppressive immune cells, and expression of co-inhibitory receptors such as PD-L1 [2]. In the last few years, targeting co-inhibitory molecules with antibodies has shown impressive results in tumor regression and overall survival, leading to the approval of anti-CTLA-4, anti-PD-1 and anti-PD-L1 in numerous cancers [3]. However, the success of immune checkpoint inhibitors (ICI) is still partial and many patients fail to respond. This is particularly true for prostate cancer (PCa), the second deadliest cancer in the industrialized world and in which numerous clinical trials using ICI monotherapy have been disappointing [4]. Limited tumor infiltrate (cold tumors) or low expression of the targeted molecule may explain the relative inefficiency of ICI [5,6]. To overcome these limitations, it is necessary to explore other pathways that might be involved in immune escape and that could complement actual therapies.

Recently, a new co-inhibitory pair has been highlighted in anti-tumor immune response: HVEM (Herpes Virus Entry Mediator, TNFRSF14) and BTLA (B and T lymphocyte attenuator) [7]. These two molecules can be expressed by many immune cells, including T-cells, in which signaling through BTLA is associated with inhibition of their activation [8,9]. Additionally, the HVEM network includes many additional partners, such as LIGHT, Herpes Simplex Virus-1 (HSV-1) glycoprotein D (gD), lymphotoxin α (LTα) or CD160 [7]. Like BTLA, binding of HVEM to CD160 on T-cells is associated with an inhibition of their activation [10]. In contrast, LIGHT is clearly a T-cell activator since transgenic expression of LIGHT in T cells leads to massive activation, especially in mucosal tissues [11]. On the other hand, stimulation of HVEM expressed by T-cells by any of its ligands is associated with proliferation, survival and production of inflammatory cytokines, such as IL-2 and IFN-γ [10,12]. Thus, the HVEM network is complex and T cell activation or inhibition may follow HVEM engagment depending on cis or trans activation by various ligands in various type of cells.

Although the role of HVEM on T cell activation is well established, much less is known on the role of HVEM expressed by tumor cells on the immune system. Several clinical studies have shown that HVEM expression is up regulated in many types of cancers including colorectal cancers [13], melanomas [14],

Preprints (www.preprints.org) | NOT PEER-REVIEWED | Posted: 13 May 2021 doi:10.20944/preprints202105.0302.v1

esophageal carcinomas [15], gastric cancers [16], hepatocarcinomas [17], breast cancers [18], lymphomas [19] or PCa [20]. In these studies, high levels of HVEM expression by tumors or soluble HVEM in the sera were associated with a worse prognosis and lower survival. Moreover, HVEM expression by tumors was also associated with a reduction in the numbers of tumor-infiltrating leukocytes (TILs) [13,15,17], indicating a detrimental role for HVEM in various cancers. Few studies have considered targeting the HVEM network to affect tumor growth. In fact, various strategies to inhibit HVEM expression or function lead to increased T cell proliferation and function in syngeneic tumor mouse models [15,21,22]. However, to our knowledge, no study to date has assessed the possibility to use a monoclonal antibody (mAb) to HVEM to favor the anti-tumor immune response in a humanized context *in vivo*.

To generate humanized mice, we used immuno-compromised NOD.SCID.γc^{null} (NSG) mice, which are deprived of murine T-, B- and NK-cells but that retain functionally immature macrophages and granulocytes [23]. Patient-Derived Xenografts (PDX) have been shown to faithfully recapitulate tumor architecture and clinical features for breast [24], ovarian [25], lung [26], skin [27] and prostate [28] cancers, for instance. However, PDX mice models are difficult to generate on a regular and consistent basis. Humanized mice grafted with human cancer cell lines have been used in hundreds of studies to evaluate various treatments efficacy for cancer immunotherapy [29]. Whatever the mode of reconstitution of immune cells (from progenitors or peripheral blood, as herein), they all suffer from the same drawback: human T cells will be allogenic to the tumor. This would prevent the tumor-antigen specific response to be faithfully recapitulated in humanized mice. Nevertheless, accumulating evidences indicate that, besides their different proportions in the native T cell repertoire, a high degree of similarity exists between the antigen-specific and allogenic-specific immune responses [30,31]. Furthermore, T cell response to the tumor is not restricted to antigen-specific T cells but can also imply bystander T cells, not specific but actively engaged in tumor control [32,33]. Thus, despite some limitations, humanized mice may still provide valuable clues on therapeutic strategies aimed at enhancing the allogenic immune response mediated by human T cells to the tumor, with relevance to T cell-mediated tumor-antigen specific and bystander immune responses in cancer patients. Herein, we investigated the therapeutic potential of a monoclonal antibody targeting human HVEM in humanized mice and the underlying cellular and molecular mechanisms associated to therapeutic efficacy.

Preprints (www.preprints.org) | NOT PEER-REVIEWED | Posted: 13 May 2021 doi:10.20944/preprints202105.0302.v1

Results

HVEM and BTLA are associated to lower progression-free intervals in prostate cancer patients

Analysis of the TCGA (The Cancer Genome Atlas) revealed that HVEM mRNA was expressed at high levels in the PRAD (PRostate ADenocarcinomas) dataset (normalized log2 counts >10) and at higher levels in primary tumors than in patient-matched normal tissues (Figure 1A). In contrast, BTLA was expressed at low (normalized log2 counts <3) and similar levels in the tumor and in the patient-matched normal tissues (Figure 1B). For patients with Gleason scores of 6 or 7 (low grade adenocarcinomas), above-median expression of HVEM was associated to a lower progression-free interval (PFI) over a 5-year period whereas this was not observed for BTLA (Figure 1C). It was the opposite in patients with more advanced disease (Gleason scores of 8 or 9), in which HVEM mRNA expression levels were not correlated with good or bad prognosis, but where above-median expression of BTLA was associated to a lower PFI (Figure 1D). Overall, above-median expression of HVEM and BTLA together was a bad PFI prognosis factor irrespective of the clinical score (Figure 1E). Interestingly, this was not observed for the PD1/PD-L1 co-inhibitory signaling pathway (Figure 1F). These results indicate a detrimental role of HVEM/BTLA in PCa at all stages of the disease and suggest that blocking the HVEM/BTLA pathway might be an interesting option for PCa patients. Accordingly, we focused the rest of the study on PCa cell lines *in vivo*.

Preprints (www.preprints.org) | NOT PEER-REVIEWED | Posted: 13 May 2021 doi:10.20944/preprints202105.0302.v1

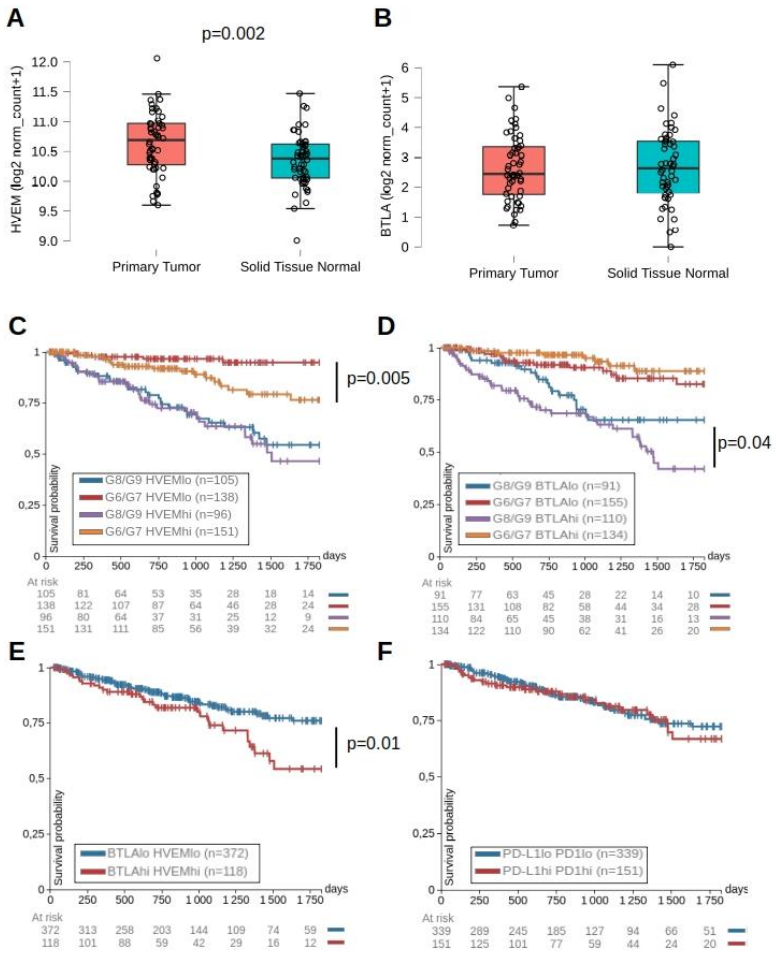

Figure 1: HVEM and BTLA are associated to lower progression-free intervals in prostate cancer patients. Expression of HVEM **(A)** and BTLA **(B)** mRNA (expressed as log2 of normalized counts) in matched patients in primary tumor or normal tissue (n=52). The p.value indicated on the graph is from a paired Student t-test with normality assumption validated by a Shapiro-Wilk test. Data were extracted from the PRAD dataset of the TCGA using Xena. Progression-free intervals (PFI) of PCa patients according to the level of expression of HVEM **(C)** or BTLA **(D)** and the Gleason scores signing low-grade (G6/G7) or high-grade (G8/G9) adenocarcinomas over a 5 year follow-up. For each group of clinical scores, patients were split into two groups according to below-median ($HVEM^{lo}$ or $BTLA^{lo}$) or above-median ($HVEM^{hi}$ or $BTLA^{hi}$) mRNA expression. PFI curves of PCa patients harboring below-median or above-median expression of both HVEM and BTLA **(E)** or both PD1 and PD-L1 **(F)** independently of clinical scores. Number of patients in each group are indicated in brackets and number of patients at risk at main time points are indicated below the graph. The p values on the graphs are from a log rank test in Xena.

Targeting HVEM with a mAb improves tumor control in humanized mice

Preprints (www.preprints.org) | NOT PEER-REVIEWED | Posted: 13 May 2021 doi:10.20944/preprints202105.0302.v1

We first determined whether targeting HVEM with a mAb could impact tumor growth *in vivo*. For that, we implanted prostate cancer cell lines in NSG mice and grafted human PBMCs few days after. No differences in tumor growth were observed in mice grafted with the prostate cancer cell line DU145, which did not express HVEM (Figure 2A). In contrast, a two fold reduction of tumor growth was observed in mice grafted with the HVEM-positive PC3 prostate cancer cell line (Figure 2B). The presence of human cells was mandatory for the efficacy of the mAb since tumor growth was unaffected by the treatment in non-humanized NSG mice (Figure S1A). The lack of an effect in non-humanized mice also indicates that the mAb did not kill directly the PC3 cell line *in vivo*. To formally demonstrate that HVEM on the tumor was required for therapeutic efficacy of the mAb, we generated an HVEM-deficient PC3 cell line (clone 1B11) using CRISPR-Cas9 ribonucleoprotein (RNP) transfection. The treatment with the mAb was completely inefficient on the 1B11 clone in humanized mice (Figure 2C), showing that HVEM expression by the tumor was mandatory for the therapeutic efficacy of the mAb. Of note is that the mAb was also effective at controlling tumor growth in humanized mice grafted with the HVEM-positive melanoma cell line Gerlach but not with the HVEM-negative breast cancer cell line MDA-MB-231 (Figure S1B-C), indicating that therapeutic efficacy of targeting HVEM was independent of the tumor tissue origin but rather strictly dependent on HVEM expression by the tumor.

Preprints (www.preprints.org) | NOT PEER-REVIEWED | Posted: 13 May 2021 doi:10.20944/preprints202105.0302.v1

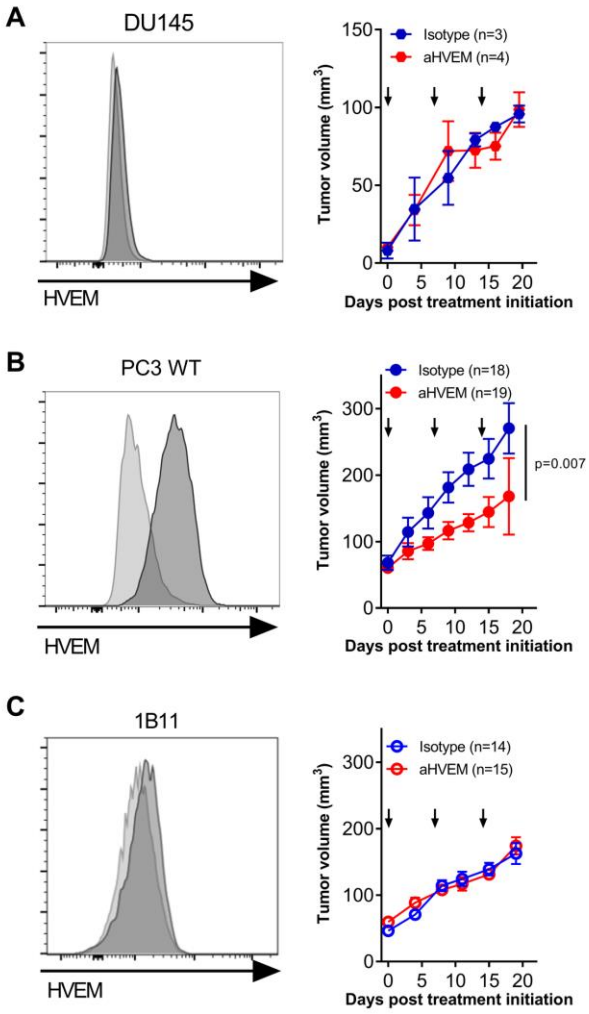

Figure 2: Targeting HVEM with a mAb improves tumor control in humanized mice. HVEM expression and tumor growth of the prostate cancer cell lines DU145 **(A)**, PC3 **(B)** and the HVEM-deficient PC3 clone 1B11 **(C)**. HVEM expression was determined by flow cytometry with the anti-HVEM mAb (clone 18.10) and a secondary antibody. Curves represent the cumulative mean tumor volume (±SEM) from one experiment with DU145, two for 1B11, and three for PC3. Numbers of mice at the beginning of the experiments are indicated in brackets. Arrows indicate the time of the injections. The p.value reported on the graph tests the null hypothesis that the slopes are identical using a linear regression model.

Tumor control is dependent on $CD8^+$ T cells

To dig into the mode of action of the mAb, we determined the composition of human $CD45^+$ cells in the PC3 tumor by flow cytometry. Human $CD3^+$ T cells represented more than 95% of $hCD45^+$ cells, in which $CD4^+$ and $CD8^+$ cells represented 40 to 60%, irrespective of the treatment (Figure S2). In contrast, we observed an increase in CD8 T cell numbers (normalized across experiments) in the anti-HVEM-treated group relative to

Preprints (www.preprints.org) | NOT PEER-REVIEWED | Posted: 13 May 2021 doi:10.20944/preprints202105.0302.v1

the control group (Figure 3A). Additionally, frequencies of cells expressing the proliferation marker Ki-67 were significantly elevated in both $CD4^+$ and $CD8^+$ T cells (Figures 3B). However, frequencies of $CD8^+$ T cells expressing both Granzyme B and Perforine-1 were not elevated (Figure 3C). To directly determine the contribution of $CD8^+$ T cells to tumor control in anti-HVEM-treated mice, we compared tumor growth in humanized mice depleted or not of human $CD8^+$ T cells. Depletion of $CD8^+$ T cells before the initiation of the treatment reverted the effect of the anti-HVEM mAb (Figure 3D), showing that tumor control was dependent on $CD8^+$ T cells.

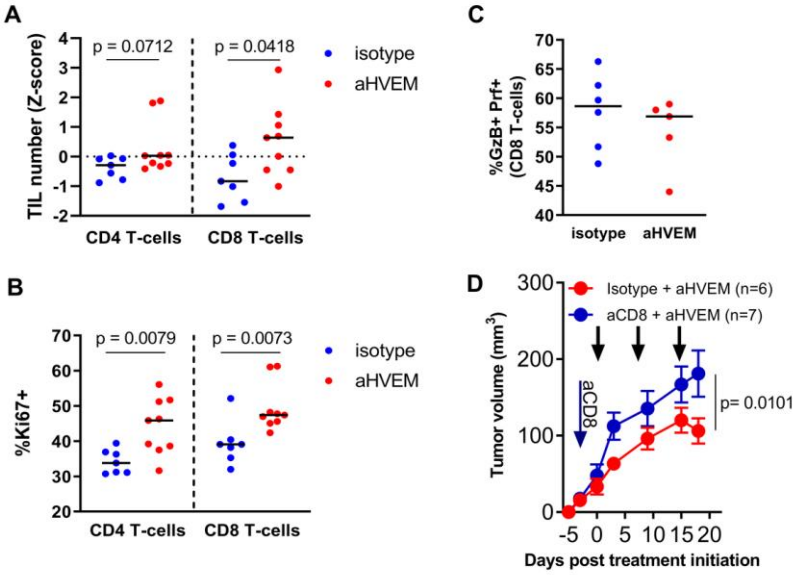

Figure 3: Tumor control is dependent on $CD8^+$ T cells. **(A)** Numbers of $CD4^+$ and $CD8^+$ T-cells in PC3 tumors from two independent experiments. To allow comparison, numbers obtained in each mice were transformed to z-scores (number of standard errors separating the samples from the mean) **(B)** Frequencies of Ki67-expressing cells among $CD4^+$ and $CD8^+$ T-cells in the tumor. Data are cumulative of two independent experiments performed at D21 post-humanization. Each dot is a mouse. The p.values on the graphs tests the null hypothesis that the median values were equals using the Mann-Whitney non parametric t-test. **(C)** Cumulative frequencies of $CD8^+$ T cells expressing Granzyme B (GzB) and Perforin (Prf) in $CD8^+$ T cells of the tumor without *ex vivo* stimulation. Data were generated in a single experiment. Tumors were analyzed 20 days after implantation. **(D)** Growth of the PC3 cell line in humanized mice treated with anti-HVEM mAb and depleted or not of their CD8 T cells. CD8 T-cells were depleted on the day following humanization (blue arrow). Curves are the mean tumor volume (±SEM) in the indicated number of mice. Black arrows indicate the time of anti-HVEM mAb injection. Data are cumulative of two independent experiments. The p value reported on the graphs tests the null hypothesis that the slopes are all identical using a linear regression model.

Preprints (www.preprints.org) | NOT PEER-REVIEWED | Posted: 13 May 2021 doi:10.20944/preprints202105.0302.v1

Treatment with the anti-HVEM mAb does not increase Graft-Vs-Host-Disease nor number or proliferation of human T cells

Our observations so far are consistent with the hypothesis that targeting HVEM on the tumor released an inhibitory signal on $CD8^+$ T cells, allowing their proliferation *in situ*. We wanted to rule out the possibility that the mAb behave as an agonist, directly activating $HVEM^+$ $CD8^+$ T cells *in vivo*, leading to better tumor control. One prediction of that hypothesis would be that GVHD occurring in NSG mice grafted with the tumor and reconstituted with human T cells would be exacerbated following anti-HVEM administration. However, despite the impact of the mAb on tumor growth (Figure 2), we observed similar weight loss and mortality in anti-HVEM or isotype control treated mice (Figure 4A-B). Furthermore, and in contrast to TILs, the activation of human T cells in the spleens were the same in both groups, as judged by similar numbers of $CD4^+$ and $CD8^+$ T cells and similar frequencies of $Ki\text{-}67^+$ cells (Figure 4C-D). Thus, anti-HVEM therapy in humanized mice reduced the growth of $HVEM^+$ tumors by a mechanism that was independent of a systemic agonist effect of the mAb on human T cells.

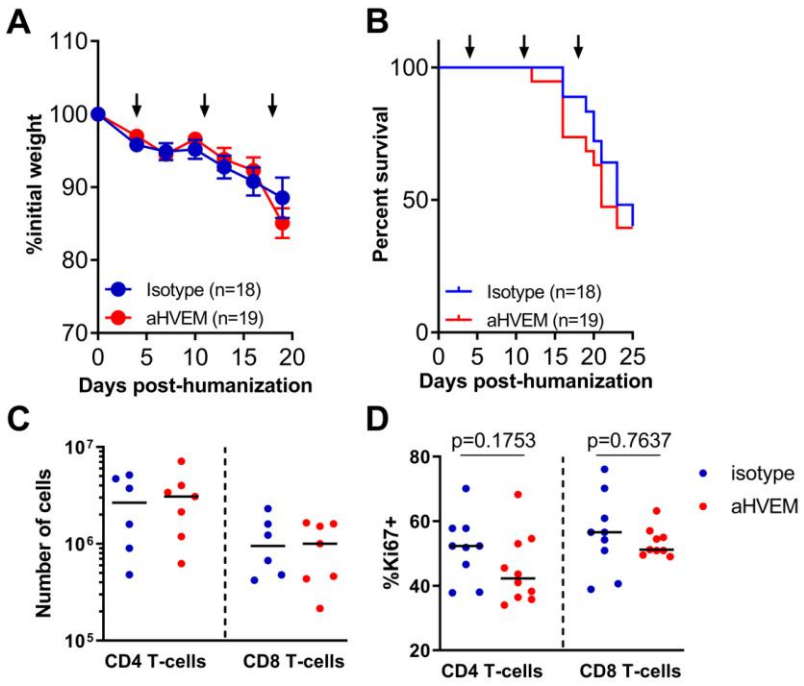

Figure 4: Treatment with the anti-HVEM mAb does not increase GVHD nor numbers or proliferation of human T cells in the spleen. Percentages of initial weight **(A)** and survival **(B)** of tumor-bearing humanized NSG mice following treatment by the anti-HVEM mAb or an isotype control are shown. Data

Preprints (www.preprints.org) | NOT PEER-REVIEWED | Posted: 13 May 2021 doi:10.20944/preprints202105.0302.v1

shown are cumulative of 3 independent experiments. Numbers **(C)** and frequencies of Ki-67$^+$ cells **(D)** at D21 post humanization in the indicated subsets and are cumulative of two independent experiments. Each dot is a mouse. The p values are from a Mann-Whitney t test.

mRNA enrichment analysis showed increased activation and decreased immuno-suppression in TILs of anti-HVEM treated mice

In order to better characterize the anti-tumor immune response following mAb treatment, we established a list of differentially expressed genes (DEG) in sorted hCD45$^+$ TILs from mice treated with the anti-HVEM mAb or its isotype control. For the analysis, 287 genes with raw count higher than 55 and an absolute fold-change of at least 20% were set to be differentially expressed. Among those 287 genes, 145 were up-regulated with a $\log_2$FC>0.26 and 142 were down-regulated ($\log_2$FC<-0.3) in HVEM-treated mice relative to isotype-treated controls (Figure 5A). Several interleukins and chemokines genes signing T cell activation were enriched in the treated group, such as *LTA*, *IL22*, *IL32*, *CCL5*, and *CCL4*. Of note, *GZMB* and *PRF1* were among the genes with the highest levels of expression but the difference between the groups was weak, confirming our observation by flow cytometry (Figure 3F). A Gene Set Enrichment Analysis (GSEA) identified the "JAK-STAT signaling pathway" signature as significantly and positively enriched in TILs of HVEM-treated mice (Figure 5B). In addition, up-regulated genes of the anti-HVEM group were enriched in members of several ontologies related to lymphocyte activation, including the tumor necrosis factor-mediated signaling pathway, cytokine and chemokine binding and activity, and T cell receptor complex (Figure S3). On the other hand, some genes belonging to immuno-suppressive pathways were clearly down-regulated in HVEM-treated TILs such as *ENTPD1* (CD39), *IL10* and the co-inhibitory receptors *BTLA*, *TIGIT*, *LAG3* and *HAVCR2* (TIM3), as well as the "don't eat me" receptor *CD47* (Figure 5A). In addition, GSEA showed that the "immunoregulatory interactions between a lymphoid and a non lymphoid cell" signature was significantly repressed in the DEG signature (Figure 5C), signing altered adhesion and motility of TILs. Overall, anti-HVEM treatment was associated with profound modifications of TILs, with an increased expression of genes belonging to activation and proliferation signaling pathways and a decreased expression of genes signing an exhausted phenotype.

Preprints (www.preprints.org) | NOT PEER-REVIEWED | Posted: 13 May 2021 doi:10.20944/preprints202105.0302.v1

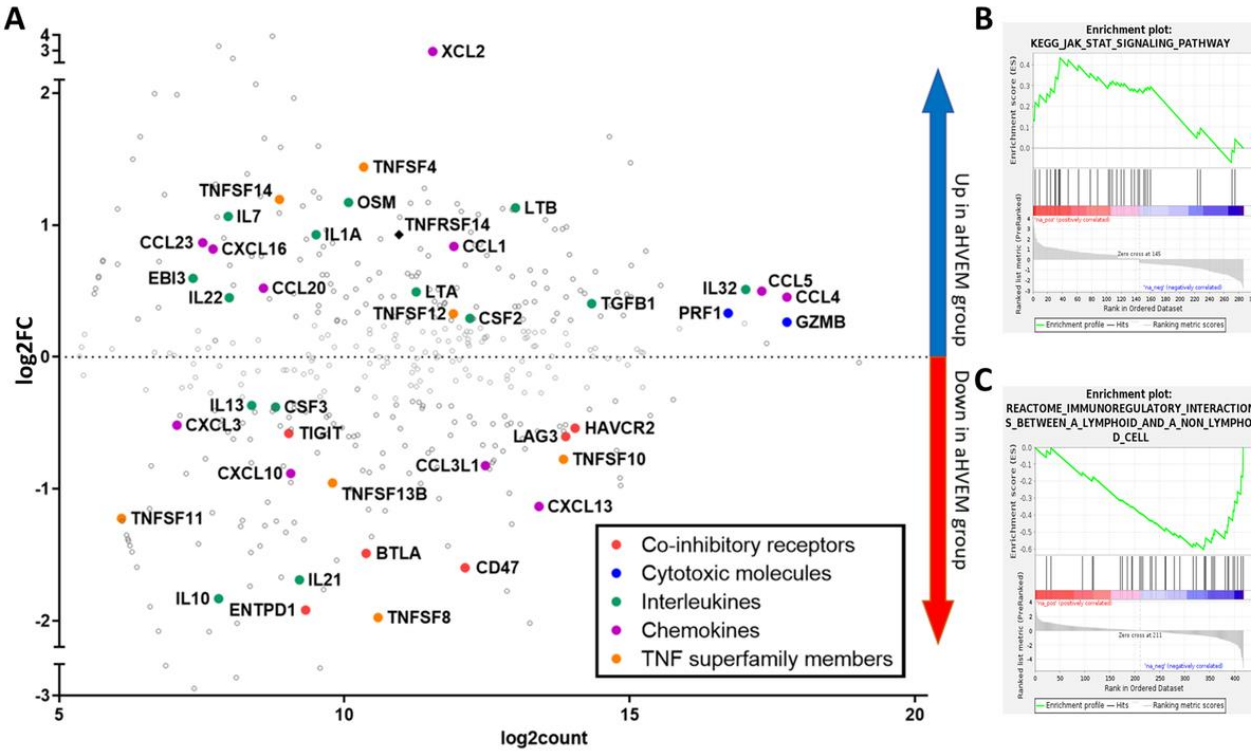

Figure 5: mRNA enrichment analysis show increased activation and decreased immunosuppression in TILs of anti-HVEM treated mice. **(A)** MA-plot comparing gene expression between TILs from aHVEM and isotype treated mice. Represented are the $\log_2$ fold-change in the expression of a given gene between anti-HVEM- or isotype-treated mice ($\log_2$FC, y axis) vs the mean absolute count after normalization ($\log_2$count). Only genes with raw counts higher than 55 are shown. Some notable genes were manually annotated according to their biological functions by the indicated color code. **(B)** GSEA identified the "JAK-STAT signaling pathway" signature as significantly enriched (Normalized Enrichment Score (NES)=1.81, p.val=0.004, q.val=0.17 (FDR), p.val=0.32 (FWER)) in genes up-regulated by the treatment. **(C)** "Immunoregulatory interaction between a lymphoid and a non lymphoid cell" signature was significantly enriched (NES=-1.86, p.val=0.001, q.val=0.15 (FDR), p.val=0.25 (FWER)) in genes down-modulated by the treatment.

HVEM is an immune checkpoint during anti-tumor T cell immune response in humanized mice

Finally, and to directly demonstrate that HVEM expression by the tumor was indeed an immune checkpoint, we devised a simple *in vivo* assay. We implanted the HVEM-positive or the HVEM-negative PC3 cells in NSG mice, and compared tumor growth with or without human PBMCs (Figure 6). Both cell lines grew equally well in non-humanized NSG mice (Figure 6A), showing that HVEM-deficiency did not impact *in*

Preprints (www.preprints.org) | NOT PEER-REVIEWED | Posted: 13 May 2021 doi:10.20944/preprints202105.0302.v1

vivo tumor development *per se*. In contrast, tumor growth of the 1B11 clone was reduced two-fold compared to the parental PC3 cell line in humanized mice (Figure 6B). Thus, removing HVEM from the tumor released a brake on the allogenic T cell response to the tumor, demonstrating that HVEM was an immune checkpoint in this experimental condition.

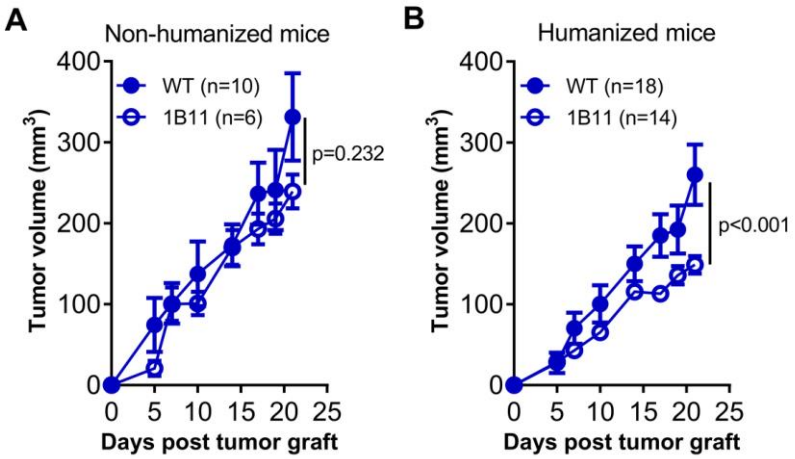

Figure 6: HVEM is an immune checkpoint during anti-tumor T cell immune response in humanized mice. Growth of the indicated PC3 cell lines (WT or 1B11) in non-humanized **(A)** or PBMC-humanized mice **(B)**. Curves are the mean tumor volume (±SEM) in the indicated number of mice. Data are cumulative of at least two experiments. The p value on the graphs indicate the probability that the slopes are equal using a linear regression model.

Discussion

Here, we report for the first time that HVEM can be targeted by a mAb to improve tumor control by human T cells *in vivo*. Moreover, we deciphered the mode of action of the mAb *in vivo* using complementary technologies. Furthermore, we developed a simple *in vivo* assay for immune checkpoint discovery and validation. To our knowledge, the present report is the first that combine CRISPR/Cas9-mediated deletion of putative checkpoints with assessment of tumor growth in humanized mice. One limitation of the assay is that PBMC-humanized mice are mostly reconstituted with T cells, as shown herein, limiting the usefulness of the assay to T cell-specific immune checkpoints. Another limitation is the allogenic nature of the immune response to the tumor in humanized mice, that would be only circumvented in PDX models with autologous

Preprints (www.preprints.org) | NOT PEER-REVIEWED | Posted: 13 May 2021 doi:10.20944/preprints202105.0302.v1

human immune cells, an ongoing effort but still difficult to set up [34]. Despite these limitatons, we believe that our simple *in vivo* assay will be of great help to investigate other candidates in more advanced models of humanized mice, i.e mice reconstituted with human hematopoietic progenitors.

We show that the HVEM/BTLA checkpoint could be exploited for therapy in humanized mice using a mAb to human HVEM. We found that HVEM expression by the tumor was necessary and sufficient to elicit tumor control by the mAb, since it had no effect on HVEM-negative cell lines and no agonist activity on human T cells. Park *et al.* showed in a syngeneic mouse model that transfecting an agonist scFv anti-HVEM in tumor cells resulted in increased T-cell proliferation, as well as improved IFN-γ and IL-2 production and better tumor control [21]. Aside the species differences, the discrepancy with our results could be explained by the fact that T-cells are strongly activated in huPBMC mice [35]. The down regulation of HVEM expression upon activation [36] may have limited the binding of the anti-HVEM antibody on T-cells in our model. Thus, it remains possible that the mAb would behave differently in humans. On the other hand, BTLA is up regulated upon T-cell activation [37], increasing the susceptibility of T-cells to inhibition by $HVEM^{+}$ tumor cells [13,15,17,38]. We observed quite the opposite in the tumor micro environment following treatment, with an increase in *HVEM* and a reduction of *BTLA* gene expression, with a concomitant increase in *LTA* and *LIGHT*, two other ligands for HVEM. It is important to note that the binding sites of LIGHT and BTLA differ on HVEM [39]. So, the anti-HVEM mAb might have limited inhibition of activated T-cells through blockade of HVEM binding with BTLA but not with the other ligands that are T-cell activators. An alternative possibility would be that LIGHT and LTA in their soluble forms inhibit the interaction of HVEM with BTLA [40]. As of today, reciprocal regulation of HVEM and BTLA has not been reported but our observation is reminiscent of earlier findings showing reciprocal regulation of HVEM by LIGHT [36].

Previous studies in mice also showed that inhibiting HVEM expression on the tumor or its interaction with its ligands has a positive effect on T cells. Injection of a plasmid encoding a soluble form of BTLA (to compete with endogenous BTLA for HVEM) was associated with an increase in inflammatory cytokines production by TILs and a decrease in anti-inflammatory cytokines at the RNA level [22]. In the same line, vaccination to a tumor-associated antigen was more efficient if HVEM interactions with its ligands were blocked by HSV-1 gD, allowing regression of large tumor mass [41]. Moreover, silencing HVEM expression in the tumor with siRNA was also associated with an increase in CD8 T cells and

inflammatory cytokine production in a murine colon carcinoma model [15]. In addition, use of siRNA to HVEM on ovarian cancer *in vitro* promoted T-cells proliferation and TNF-α and IFN-γ production [42]. Numerous results from our study also support increased T cell activation in the absence of HVEM/BTLA signaling: TILs from mice treated with anti-HVEM were enriched in ontologies signing activation by cytokines, chemokines and signaling pathways that are well known inducers of proliferation, differentiation, migration and apoptosis. Comparison between TILs from mice treated with the anti-HVEM or isotype control mAb also highlighted decreased expression of many co-inhibitory receptors genes (*BTLA*, *TIGIT*, *LAG3*, and *HAVCR2* [43,44]) or with immunosuppressive functions (*ENTPD1* and *IL10*), suggesting a lower exhaustion status. Overall, we propose a model in which treatment with the anti-HVEM mAb would block the BTLA-associated inhibitory signaling on $CD8^+$ TILs that would increased their proliferation and numbers, reduced their exhausted phenotype and improved their migration and/or adhesion to the tumor, ultimately leading to better tumor control.

Conclusions

The recent success of ICI for cancer immunotherapy (anti-CTLA-4, anti-PD-1/PD-L1) has confirmed the hypothesis that the immune system can control many cancers but disappointing results were obtained for PCa [4], in line with our observation that PD1/PD-L1 are not associated to lower PFI in PCa patients. In light of the promising results reported herein, anti-HVEM therapy might be combined with ICI and/or chemotherapy to further enhance anti-tumor immunity in PCa.

Preprints (www.preprints.org) | NOT PEER-REVIEWED | Posted: 13 May 2021 doi:10.20944/preprints202105.0302.v1

Materials and Methods

Preparation of human peripheral mononuclear cells

Human peripheral blood was obtained from Etablissement Francais du Sang (EFS) after informed consent of the donor. Human peripheral blood mononuclear cells (PBMC) were isolated on a density gradient (Biocoll). Cells were washed in PBS 3% FCS and diluted at the appropriate concentration in 1X PBS before injection into mice.

Humanized mice tumor model

All animals used were NSG mice (stock ≠005557) purchased from the Jackson Laboratory (USA). To assess therapeutic activity, 8–20-week-old NSG mice (males and females) were injected subcutaneously with 2.10^6 tumor cells. One week later, mice were irradiated (2 Gy) and grafted the same day with 2.10^6 huPBMC by retro orbital injection. Four to 5 days after transplantation, the anti-huHVEM antibody or isotype control was injected intra-peritoneally at 2 mg/kg. General state, body weight and survival of mice were monitored every 3-4 days to evaluate Graft-vs-Host-Disease (GVHD) progression. Mice were euthanized when exhibiting signs of GVHD, such as hunched back, ruffled fur, and reduced mobility. For CD8 depletion, mice were injected intra-peritoneally with 10mg/kg of the anti-CD8 MT807R1(Rhesus recombinant IgG1 provided by the Nonhuman Primate Reagent Resource [45]) or the isotype control (clone DSPR1) the day following humanization.

Antibodies

The clone 18.10 has been described previously [46]. Briefly, 18.10 is a murine IgG1 anti-human HVEM mAb and was produced as ascites and purified by protein A binding and elution with the Affi-gel Protein A MAPS II Kit (Bio-rad). A mouse IgG1 isotype control (clone MOPC-21 clone) was purchased from Bio X Cell (West Lebanon, NH, USA).

Cell lines

PC3 (non-hormonal-dependent human prostate cancer cells) and DU145 (prostate cancer cells) were grown in high glucose DMEM media supplemented with 10% FCS, L-glutamine and antibiotics (Penicillin/Streptomycin). The PC3 cell line was genetically authenticated before the initiation of the

experiments (Eurofins). All cells were confirmed to be free of mycoplasmas before injection into mice by the MycoAlert detection kit (Lonza). Tumor growth was monitored using an electronic caliper and volumes were determined using the following formula: [(length*width²)/2].

Generation of HVEM deficient PC3 clone using CRISPR-Cas9 RNP transfection

50,000 PC3 cells were seeded in a 24-well plate. Twenty-four hours later, cells were incubated with sgRNA complementary to exon 3 of HVEM (GCCAUUGAGGUGGGCAAUGU + Scaffold, TrueGuide Synthtetic guide RNAs, Invitrogen™), Cas9 nuclease (TrueCut™ Cas9 Protein v2, Invitrogen™) and lipofectamine (Lipofectamine™ CRISPRMAX™ Cas9 Transfection Reagent, Invitrogen™) according to manufacturer instructions (TrueCut Cas9 protein v2 (27/09/2017)). After three days, efficiency was evaluated with GeneArt Genomic Cleavage Detection Kit (Invitrogen™) according to the manufacturer instructions. For this assay, DNA was amplified with the following primers: TGCGAAGTTCCCACTCTCTG (Forward) and GGATAAGGGTCAGTCGCCAA (Reverse). Cells were cloned by limiting dilution in 96-well plates. Clones were screened for HVEM expression by flow cytometry using anti-HVEM (clone 94801, BD) and were considered as negative if HVEM expression was undetectable for at least 3 subsequent measurements.

Phenotypic analysis by flow cytometry

Tumors were digested with 0.84mg/mL of collagenase IV and 10µg/mL DNAse I (Sigma Aldrich) for 40min at 37°C with an intermediate flushing of the tissue. Cells were passed through a 100µm-cell strainer and suspended in PBS 3% FCS. To eliminate dead cells and debris, tumor cell suspensions were isolated on a Biocoll gradient. Rings were collected, washed, and cell pellets were suspended in PBS 3% FCS before counting on LUNA™ Automated Cell counter (Logos Biosystems). Subsequently, up to 2.10^6 live cells were stained with viability dye (eF506, Fixable Viability Dye, ThermoFisher) for 12 min. at 4°C, Fc receptor were blocked with human FcR Blocking Reagent (120-000-442, Miltenyi Biotec) and anti-CD16/32 (clone 2.4G2) for 10 min. The followings antibodies were added for 35 min. at 4°C: hCD45-BUV805 (HI30, BD), hCD3-PECyn7 (SK7, BD), hCD4-PerCP (RPA-T4, Biolegend), hCD8-APC-H7 (SK1, BD), hKi67-AF700 (B56, BD), hCD270-BV421 (cw10, BD), mCD45-BUV395 (30-F11, BD), hGranzymeB-APC (GB11, eBioscience), and hPerforin-PE (B-D48, Biolegend). For intracellular staining, Foxp3/Transcription Factor Staining (eBioscience) or Cytofix/Cytoperm (BD) buffer sets were used. Cells were washed with 1X PBS before acquisition on an X20 cytometer (Becton Dickinson (BD), San Jose, CA). The absolute count of different

populations was determined by adding 50 µL of Cell Counting Beads (Bangs Laboratories) before acquisition. Data were analyzed using FlowJo software (TreeStar, Ashland, OR, USA).

NanoString nCounter expression assay

For Nanostring® experiment, 14 to 15 weeks-old NSG mice were humanized and treated with anti-HVEM or isotype. Day 28 post humanization, tumors were harvested and TILs were isolated as described above. To maximize mRNA recovery, TILs were pooled by treatment groups (4 mice in the anti-HVEM group and 5 in the isotype control group). Then, cells were stained with viability dye (eF506) and anti hCD45-APC (HI30, Biolegend). Live $hCD45^+$ cells were sorted using Aria II cell sorter. After centrifugation, cells were suspended in RLT buffer (Qiagen) before freezing at -80°C until analysis. Data were normalized through the use of NanoString's intrinsic negative and positive controls according to the normalization approach of the nSolver analysis software (Nanostring).

Bioinformatics analysis

For ontologies enrichment analysis, only genes up regulated by the treatment were analyzed using the enrichment analysis visualization Appyter to visualize Enrichr results [47] . DEG (up- an down-regulated) were ranked by fold-change for pre-ranked GSEA. Enrichment was performed with the C2 Canonical Pathways v7.4 gene set using the GSEA 4.1.0 Linux desktop application [48]from the Broad Institute. With that workflow, a False Discovery Rate (FDR) or a Family Wise Error Rate (FWER) less than 0.25 is deemed "significant". The Cancer Genome Atlas (TCGA) database was interrogated using the Xena browser ((http://xena.ucsc.edu) provided by the University of California (Santa Cruz, CA, USA) [49]. The Prostate Adenocarcinoma (PRAD) dataset was used with subsequent filterings on TNFRSF14, BTLA, PDCD1, and CD274 mRNA expression levels and Gleason clinical scores.

Statistical analysis

All statistical tests were performed with Prism v8 (Graph Pad Inc, La Jolla, CA, USA) or JASP v0.14.3 (available at https://jasp-stats.org). The nature of the statistical test used to compare results is indicated in each legend of the figures. When necessary, the p-values of these tests are indicated on the figure panels. Statistical power of the analyses (alpha) was arbitrarily set at 0.05. No test was performed *a priori* to adequate the number of samples with statistical power.

Preprints (www.preprints.org) | NOT PEER-REVIEWED | Posted: 13 May 2021 doi:10.20944/preprints202105.0302.v1

Supplementary materials

Figure S1: Anti-HVEM therapy in humanized mice.

Figure S2: T cell landscape in PC3 tumor of humanized mice.

Figure S3: Enrichment analysis in TILs of anti-HVEM-treated mice.

Abbreviations

PBMC, Peripheral Blood Mononucelar Cells; HVEM, Herpes Virus Entry Mediator; BTLA, B and T Lymphocyte Attenuator; TILs, Tumor-Infltrating Leukocytes; NSG, NOD.SCID.γc-null; ICI, Immune Checkpoint Inhibitors; RNP, ribonucleoproteins; DEG, Differentially Expressed Genes; GVHD, Graft-Vs-Host-Disease; IPA, Ingenuity Pathway Analysis; GSEA, Gene Set Enrichment Analysis; FDR, False Discovery Rate; FWER, Family Wise Error Rate; PDX, Patient-Derived Xenografts; PCa, Prostate Cancer; TCGA, The Cancer Genome Atlas; PRAD, Prostate Adenocarcinomas; PFI, Progression-Free Interval

Declarations

Ethics approval and consent to participate

Human peripheral blood mononuclear cells were collected by Etablissement Français du Sang from healthy adult volunteers after informed consent in accordance with the Declaration of Helsinki. Mice were bred in our animal facility under specific pathogen-free conditions in accordance with current European legislation. All protocols were approved by the Ethics Committee for Animal Experimentation Charles Darwin (Ce5/2012/025).

Consent for publication: All authors concur with the submission of the article in its present form

Competing interests: DO declares competing interests as being the co-founder and shareholder of Imcheck Therapeutics, Alderaan Biotechnology and Emergence Therapeutics and has research funds from Imcheck Therapeutics, Alderaan Biotechnology, Cellectis and Emergence Therapeutics.

Funding

This study was supported by INSERM Transfert, Cancéropôle Île-de-France and Association pour la recherche sur les Tumeurs de la Prostate (ARTP). The funders play no role in the design of the study and collection, nor in the analysis or interpretation of the data. S.B. was supported by a doctoral fellowship from the French Ministère de l'Education Supérieure et de la Recherche. N.A. is supported by a doctoral

fellowship from the Fondation Association pour la Recherche sur le Cancer (ARC). D.O.'s team was supported by the grant "Equipe FRM DEQ201802339209". D.O. is Senior Scholar of the Institut Universitaire de France.

Authors' contributions

SB and NA performed the experiments, analyzed the data and contributed to the writing of the manuscript, DO provided essential reagents and edited the manuscript, GM designed the study, analyzed the data and wrote the manuscript.

Acknowledgments

The authors would like to thank Olivier Bregerie, Flora Issert and Doriane Foret for taking care of our mice, Dr Pukar KC for technical help, Sylvaine Just-Landi for preparing the 18.10 mAb, Armanda Casrouge and Claude Baillou for cell sorting, and Dr Benoit Salomon for critical reading of the manuscript. The results shown here are part based upon data generated by the TCGA Research Network: https://www.cancer.gov/tcga.

References

1. Hanahan, D.; Weinberg, R.A. Hallmarks of cancer: The next generation. *Cell* **2011**, *144*, 646–674, doi:10.1016/j.cell.2011.02.013.
2. Mittal, D.; Gubin, M.M.; Schreiber, R.D.; Smyth, M.J. New insights into cancer immunoediting and its three component phases-elimination, equilibrium and escape. *Curr. Opin. Immunol.* **2014**, *27*, 16–25, doi:10.1016/j.coi.2014.01.004.
3. Hargadon, K.M.; Johnson, C.E.; Williams, C.J. Immune checkpoint blockade therapy for cancer: An overview of FDA-approved immune checkpoint inhibitors. *Int. Immunopharmacol.* **2018**, *62*, 29–39, doi:10.1016/j.intimp.2018.06.001.
4. Kim, T.J.; Koo, K.C. Current status and future perspectives of checkpoint inhibitor immunotherapy for prostate cancer: A comprehensive review. *Int. J. Mol. Sci.* 2020, *21*, 1–16.
5. Havel, J.J.; Chowell, D.; Chan, T.A. The evolving landscape of biomarkers for checkpoint inhibitor immunotherapy. *Nat. Rev. Cancer* **2019**, *19*, 133, doi:10.1038/s41568-019-0116-x.
6. Park, Y.-J.; Kuen, D.-S.; Chung, Y. Future prospects of immune checkpoint blockade in cancer: from response prediction to overcoming resistance. *Exp. Mol. Med.* **2018**, *50*, 109, doi:10.1038/s12276-018-0130-1.

7. Pasero, C.; Speiser, D.E.; Derré, L.; Olive, D. The HVEM network: new directions in targeting novel costimulatory/co-inhibitory molecules for cancer therapy. *Curr. Opin. Pharmacol.* **2012**, *12*, 478–85, doi:10.1016/j.coph.2012.03.001.

8. Cai, G.; Anumanthan, A.; Brown, J. a; Greenfield, E. a; Zhu, B.; Freeman, G.J. CD160 inhibits activation of human CD4+ T cells through interaction with herpesvirus entry mediator. *Nat. Immunol.* **2008**, *9*, 176–185, doi:10.1038/ni1554.

9. Sedy, J.R.; Gavrieli, M.; Potter, K.G.; Hurchla, M. a; Lindsley, R.C.; Hildner, K.; Scheu, S.; Pfeffer, K.; Ware, C.F.; Murphy, T.L.; et al. B and T lymphocyte attenuator regulates T cell activation through interaction with herpesvirus entry mediator. *Nat. Immunol.* **2005**, *6*, 90–98, doi:10.1038/ni1144.

10. Cheung, T.C.; Steinberg, M.W.; Oborne, L.M.; Macauley, M.G.; Fukuyama, S.; Sanjo, H.; D'Souza, C.; Norris, P.S.; Pfeffer, K.; Murphy, K.M.; et al. Unconventional ligand activation of herpesvirus entry mediator signals cell survival. *Proc. Natl. Acad. Sci. U. S. A.* **2009**, *106*, 6244–6249, doi:10.1073/pnas.0902115106.

11. Shaikh, R.B.; Santee, S.; Granger, S.W.; Butrovich, K.; Cheung, T.; Kronenberg, M.; Cheroutre, H.; Ware, C.F. Constitutive Expression of LIGHT on T Cells Leads to Lymphocyte Activation, Inflammation, and Tissue Destruction. *J. Immunol.* **2001**, *167*, 6330–6337, doi:10.4049/jimmunol.167.11.6330.

12. Harrop, J.A.; McDonnell, P.C.; Brigham-Burke, M.; Lyn, S.D.; Minton, J.; Tan, K.B.; Dede, K.; Spampanato, J.; Silverman, C.; Hensley, P.; et al. Herpesvirus entry mediator ligand (HVEM-L), a novel ligand for HVEM/TR2, stimulates proliferation of T cells and inhibits HT29 cell growth. *J. Biol. Chem.* **1998**, *273*, 27548–27556, doi:10.1074/jbc.273.42.27548.

13. Inoue, T.; Sho, M.; Yasuda, S.; Nishiwada, S.; Nakamura, S.; Ueda, T.; Nishigori, N.; Kawasaki, K.; Obara, S.; Nakamoto, T.; et al. HVEM Expression Contributes to Tumor Progression and Prognosis in Human Colorectal Cancer. *Anticancer Res.* **2015**, *35*, 1361–1367.

14. Malissen, N.; Macagno, N.; Granjeaud, S.; Granier, C.; Moutardier, V.; Gaudy-Marqueste, C.; Habel, N.; Mandavit, M.; Guillot, B.; Pasero, C.; et al. HVEM has a broader expression than PD-L1 and constitutes a negative prognostic marker and potential treatment target for melanoma. *Oncoimmunology* **2019**, *8*, doi:10.1080/2162402X.2019.1665976.

15. Migita, K.; Sho, M.; Shimada, K.; Yasuda, S.; Yamato, I.; Takayama, T.; Matsumoto, S.; Wakatsuki, K.; Hotta, K.; Tanaka, T.; et al. Significant involvement of herpesvirus entry mediator in human esophageal squamous cell carcinoma. *Cancer* **2014**, *120*, 808–817, doi:10.1002/cncr.28491.

16. Lan, X.; Li, S.; Gao, H.; Nanding, A.; Quan, L.; Yang, C.; Ding, S.; Xue, Y. Increased BTLA and HVEM in gastric cancer are associated with progression and poor prognosis. *Onco. Targets. Ther.* **2017**, *10*, 919–926, doi:10.2147/OTT.S128825.

17. Hokuto, D.; Sho, M.; Yamato, I.; Yasuda, S.; Obara, S.; Nomi, T.; Nakajima, Y. Clinical impact of herpesvirus entry mediator expression in human hepatocellular carcinoma. *Eur. J. Cancer* **2015**, *51*, 157–165, doi:10.1016/j.ejca.2014.11.004.

18. Tsang, J.Y.S.; Chan, K.-W.; Ni, Y.-B.; Hlaing, T.; Hu, J.; Chan, S.-K.; Cheung, S.-Y.; Tse, G.M. Expression and Clinical Significance of Herpes Virus Entry Mediator (HVEM) in Breast Cancer. *Ann. Surg. Oncol.* **2017**, *24*, 4042–4050, doi:10.1245/s10434-017-5924-1.

19. M'Hidi, H.; Thibult, M.L.; Chetaille, B.; Rey, F.; Bouadallah, R.; Nicollas, R.; Olive, D.; Xerri, L. High expression of the inhibitory receptor BTLA in T-follicular helper cells and in B-cell small lymphocytic lymphoma/chronic lymphocytic leukemia. *Am. J. Clin. Pathol.* **2009**, *132*, 589–596, doi:10.1309/AJCPPHKGYYGGL39C.

20. Wang, Q.; Ye, Y.; Yu, H.; Lin, S.-H.; Tu, H.; Liang, D.; Chang, D.W.; Huang, M.; Wu, X. Immune checkpoint-related serum proteins and genetic variants predict outcomes of localized prostate cancer, a cohort study. *Cancer Immunol. Immunother.* **2020**, doi:10.1007/s00262-020-02718-1.

21. Park, J.-J.; Anand, S.; Zhao, Y.; Matsumura, Y.; Sakoda, Y.; Kuramasu, A.; Strome, S.E.; Chen, L.; Tamada, K. Expression of anti-HVEM single-chain antibody on tumor cells induces tumor-specific immunity with long-term memory. *Cancer Immunol. Immunother.* **2012**, *61*, 203–214, doi:10.1007/s00262-011-1101-8.

22. Han, L.; Wang, W.; Fang, Y.; Feng, Z.; Liao, S.; Li, W.; Li, Y.; Li, C.; Maitituoheti, M.; Dong, H.; et al. Soluble B and T Lymphocyte Attenuator Possesses Antitumor Effects and Facilitates Heat Shock Protein 70 Vaccine-Triggered Antitumor Immunity against a Murine TC-1 Cervical Cancer Model In Vivo. *J. Immunol.* **2009**, *183*, 7842–7850, doi:10.4049/jimmunol.0804379.

23. Shultz, L.D.; Schweitzer, P.A.; Christianson, S.W.; Gott, B.; Schweitzer, I.B.; Tennent, B.; McKenna, S.; Mobraaten, L.; Rajan, T. V; Greiner, D.L. Multiple defects in innate and adaptive immunologic function in NOD/LtSz-scid mice. *J Immunol* **1995**, *154*, 180–91.

24. DeRose, Y.S.; Wang, G.; Lin, Y.-C.; Bernard, P.S.; Buys, S.S.; Ebbert, M.T.W.; Factor, R.; Matsen, C.; Milash, B.A.; Nelson, E.; et al. Tumor grafts derived from women with breast cancer authentically reflect tumor pathology, growth, metastasis and disease outcomes. *Nat Med* **2011**, *17*, 1514–1520, doi:http://www.nature.com/nm/journal/v17/n11/abs/nm.2454.html#supplementary-information.

25. Bankert, R.B.; Balu-Iyer, S. V.; Odunsi, K.; Shultz, L.D.; Kelleher, R.J.; Barnas, J.L.; Simpson-Abelson, M.; Parsons, R.; Yokota, S.J. Humanized mouse model of ovarian cancer recapitulates patient solid tumor progression, ascites formation, and metastasis. *PLoS One* **2011**, *6*, e24420, doi:10.1371/journal.pone.0024420.

26. Chen, X.; Shen, C.; Wei, Z.; Zhang, R.; Wang, Y.; Jiang, L.; Chen, K.; Qiu, S.; Zhang, Y.; Zhang, T.; et al. Patient-derived non-small cell lung cancer xenograft mirrors complex tumor heterogeneity. *Cancer Biol. Med.* **2021**, *18*, 184–198, doi:10.20892/j.issn.2095-3941.2020.0012.

27. Quintana, E.; Piskounova, E.; Shackleton, M.; Weinberg, D.; Eskiocak, U.; Fullen, D.R.; Johnson, T.M.; Morrison, S.J. Human melanoma metastasis in NSG mice correlates with clinical outcome in patients. *Sci. Transl. Med.* **2012**, *4*, 159ra149, doi:10.1126/scitranslmed.3004599.

28. Rea, D.; Del Vecchio, V.; Palma, G.; Barbieri, A.; Falco, M.; Luciano, A.; De Biase, D.; Perdonà, S.; Facchini, G.; Arra, C. Mouse Models in Prostate Cancer Translational Research: From Xenograft to PDX. *Biomed Res. Int.* **2016**, *2016*, doi:10.1155/2016/9750795.

29. De La Rochere, P.; Guil-Luna, S.; Decaudin, D.; Azar, G.; Sidhu, S.S.; Piaggio, E. Humanized Mice for the Study of Immuno-Oncology. *Trends Immunol.* 2018, *39*, 748–763.

30. Wang, Y.; Singh, N.K.; Spear, T.T.; Hellman, L.M.; Piepenbrink, K.H.; McMahan, R.H.; Rosen, H.R.; Vander Kooi, C.W.; Nishimura, M.I.; Baker, B.M. How an alloreactive T-cell receptor achieves peptide and MHC specificity. *Proc. Natl. Acad. Sci. U. S. A.* **2017**, *114*, E4792–E4801, doi:10.1073/pnas.1700459114.

31. Felix, N.J.; Allen, P.M. Specificity of T-cell alloreactivity. *Nat. Rev. Immunol.* 2007, *7*, 942–953.

32. Kearney, C.J.; Vervoort, S.J.; Hogg, S.J.; Ramsbottom, K.M.; Freeman, A.J.; Lalaoui, N.; Pijpers, L.; Michie, J.; Brown, K.K.; Knight, D.A.; et al. Tumor immune evasion arises through loss of TNF sensitivity. *Sci. Immunol.* **2018**, *3*, eaar3451, doi:10.1126/sciimmunol.aar3451.

33. Simoni, Y.; Becht, E.; Fehlings, M.; Loh, C.Y.; Koo, S.; Teng, K.W.W.; Yeong, J.P.S.; Nahar, R.; Zhang, T.; Kared, H.; et al. Bystander CD8+ T cells are abundant and phenotypically distinct in human tumour infiltrates. *Nature* **2018**, *557*, 575–579, doi:10.1038/s41586-018-0130-2.

34. Jespersen, H.; Lindberg, M.F.; Donia, M.; Söderberg, E.M.V.; Andersen, R.; Keller, U.; Ny, L.; Svane, I.M.; Nilsson, L.M.; Nilsson, J.A. Clinical responses to adoptive T-cell transfer can be modeled in an autologous immune-humanized mouse model. *Nat. Commun.* **2017**, *8*, 1–10, doi:10.1038/s41467-017-00786-z.

35. Ali, N.; Flutter, B.; Rodriguez, R.S.; Sharif-Paghaleh, E.; Barber, L.D.; Lombardi, G.; Nestle, F.O. Xenogeneic Graft-versus-Host-Disease in NOD-scid IL- 2Rcnull Mice Display a T-Effector Memory Phenotype. *PLoS One* **2012**, *7*, 10.

36. Morel, Y.; Schiano de Colella, J.-M.; Harrop, J.; Deen, K.C.; Holmes, S.D.; Wattam, T.A.; Khandekar, S.S.; Truneh, A.; Sweet, R.W.; Gastaut, J.-A.; et al. Reciprocal Expression of the TNF Family Receptor Herpes Virus Entry Mediator and Its Ligand LIGHT on Activated T Cells: LIGHT Down-Regulates Its Own Receptor. *J. Immunol.* **2000**, *165*, 4397–4404, doi:10.4049/jimmunol.165.8.4397.

37. Murphy, K.M.; Nelson, C.A.; Šedý, J.R. Balancing co-stimulation and inhibition with BTLA and HVEM. *Nat. Rev. Immunol.* **2006**, *6*, 671–681, doi:10.1038/nri1917.

38. Sasaki, Y.; Hokuto, D.; Inoue, T.; Nomi, T.; Yoshikawa, T.; Matsuo, Y.; Koyama, F.; Sho, M. Significance of Herpesvirus Entry Mediator Expression in Human Colorectal Liver Metastasis. *Ann. Surg. Oncol.* **2019**, *26*, 3982–3989, doi:10.1245/s10434-019-07625-z.

39. Compaan, D.M.; Gonzalez, L.C.; Tom, I.; Loyet, K.M.; Eaton, D.; Hymowitz, S.G. Attenuating lymphocyte activity: The crystal structure of the BTLA-HVEM complex. *J. Biol. Chem.* **2005**, *280*, 39553–39561, doi:10.1074/jbc.M507629200.

40. Steinberg, M.W.; Cheung, T.C.; Ware, C.F. The signaling networks of the herpesvirus entry mediator (TNFRSF14) in immune regulation. *Immunol. Rev.* **2011**, *244*, 169–187, doi:10.1111/j.1600-065X.2011.01064.x.

41. Lasaro, M.O.; Sazanovich, M.; Giles-Davis, W.; Mrass, P.; Bunte, R.M.; Sewell, D.A.; Hussain, S.F.; Fu, Y.-X.; Weninger, W.; Paterson, Y.; et al. Active Immunotherapy Combined With Blockade of a Coinhibitory Pathway Achieves Regression of Large Tumor Masses in Cancer-prone Mice. *Mol. Ther.* **2011**, *19*, 1727–1736, doi:10.1038/mt.2011.88.

42. Zhang, T.; Ye, L.; Han, L.; He, Q.; Zhu, J. Knockdown of HVEM, a Lymphocyte Regulator Gene, in Ovarian Cancer Cells Increases Sensitivity to Activated T Cells. *Oncol. Res. Featur. Preclin. Clin. Cancer Ther.* **2016**, *24*, 189–196, doi:10.3727/096504016X14641336229602.

43. Anderson, A.C.; Joller, N.; Kuchroo, V.K. Lag-3, Tim-3, and TIGIT: Co-inhibitory Receptors with Specialized Functions in Immune Regulation. *Immunity* **2016**, *44*, 989–1004, doi:10.1016/j.immuni.2016.05.001.

44. De Sousa Linhares, A.; Leitner, J.; Grabmeier-Pfistershammer, K.; Steinberger, P. Not All Immune Checkpoints Are Created Equal. *Front. Immunol.* **2018**, *9*, doi:10.3389/fimmu.2018.01909.

45. Schmitz, J.E.; Simon, M.A.; Kuroda, M.J.; Lifton, M.A.; Ollert, M.W.; Vogel, C.W.; Racz, P.; Tenner-Racz, K.; Scallon, B.J.; Dalesandro, M.; et al. A nonhuman primate model for the selective elimination of CD8+ lymphocytes using a mouse-human chimeric monoclonal antibody. *Am J Pathol* **1999**, *154*, 1923–1932, doi:S0002-9440(10)65450-8 [pii]10.1016/S0002-9440(10)65450-8.

46. Gertner-Dardenne, J.; Fauriat, C.; Orlanducci, F.; Thibult, M.L.; Pastor, S.; Fitzgibbon, J.; Bouabdallah, R.; Xerri, L.; Olive, D. The co-receptor BTLA negatively regulates human Vg9Vd2 T-cell proliferation: A potential way of immune escape for lymphoma cells. *Blood* **2013**, *122*, 922–931, doi:10.1182/blood-2012-11-464685.

47. Xie, Z.; Bailey, A.; Kuleshov, M. V.; Clarke, D.J.B.; Evangelista, J.E.; Jenkins, S.L.; Lachmann, A.; Wojciechowicz, M.L.; Kropiwnicki, E.; Jagodnik, K.M.; et al. Gene Set Knowledge Discovery with Enrichr. *Curr. Protoc.* **2021**, *1*, e90, doi:10.1002/cpz1.90.

48. Subramanian, A.; Kuehn, H.; Gould, J.; Tamayo, P.; Mesirov, J.P. GSEA-P: A desktop application for gene set enrichment analysis. *Bioinformatics* **2007**, *23*, 3251–3253, doi:10.1093/bioinformatics/btm369.

49. Goldman, M.J.; Craft, B.; Hastie, M.; Repečka, K.; McDade, F.; Kamath, A.; Banerjee, A.; Luo, Y.; Rogers, D.; Brooks, A.N.; et al. Visualizing and interpreting cancer genomics data via the Xena platform. *Nat. Biotechnol.* **2020**, *38*, 675–678, doi:10.1038/s41587-020-0546-8.